Eighth International Conference on
STEEL AND ALUMINIUM STRUCTURES
Edited by B. Young & Y. Cai
Hong Kong, China, December 7 – 9, 2016

DESIGN OF STEEL-CONCRETE-STEEL SANDWICH COMPOSITE SHELL STRUCTURES

Zhenyu HUANG[a], J.Y. Richard LIEW[b]

[a] Department of Civil and Environmental Engineering, National University of Singapore, Singapore
Emails: ceehzh@nus.edu.sg, ceeljy@nus.edu.sg

[b] School of Civil Engineering, Nanjing Tech University, Jiangsu, China

Keywords: Design methodology; Floating concrete; Lightweight concrete; Sandwich structures; Sandwich shell; Ultimate strength.

Abstract. *This paper presents the latest research and development work related to steel-concrete-steel (SCS) sandwich composite shell structures for the use as Arctic region to resist ice impact loads. The main innovation of the research is the development of ultra-lightweight cement composite that is lighter than the density of water for use as infilled material for the proposed sandwich structure. The cement composite core material is held together with the two steel plates by mechanical connectors to form composite shell to resist extreme loads caused by floating ice. A series of tests on the sandwich shells subject to patch load has been carried out. The structural performance of the sandwich shells is evaluated. Design methods including guideline of connector spacing, rise-to-span ratio and span-to-thickness ratio are recommended to prevent local buckling of steel plate and to ensure structural integrity of the sandwich shell subject to concentrated loads.*

1 RECENT INNOVATION ON SANDWICH COMPOSITE STRUCTURES

Steel-concrete-steel (SCS) sandwich composite structure comprises of two external steel plates with a concrete core filled in between them (Figure 1). The composite action between the steel and concrete core is achieved by using mechanical connectors. The SCS sandwich composite exhibits significant structural and economic advantages over the conventional reinforced concrete structures in terms of higher flexural stiffness and energy absorption capacity to withstand extreme environmental and accidental loads. The external steel plates may serve as a permanent formwork during concreting, promoting construction efficiency and reducing the site handling costs and time. The waterproof feature inherently provided by external steel plates reduces surface area that needs expensive corrosive protection and makes it easy for inspection and maintenance. For conventional stiffened steel structure, plate buckling usually governed the ultimate strength so that much welding of stiffeners are needed to reduce the effective width of the plates. Large corrosion surface will be generated if using stiffened plates so that needs expensive corrosive protection. Moreover, fatigue issue becomes more pronounced issue due to much welding. Weldability issue should be addressed if high tensile strength steel and thick steel plates are used.

SCS sandwich concept reduces welding work, improve the construction efficiency and promote the structural performance which is strongly recommended to be adopted as heavy duty and protective layers such as ice-resisting walls in Arctic offshore, ship hulls, tunnels,

military shelters and nuclear power station walls that require resistance against extreme loads [1-3].

Weight can be reduced if using lightweight concrete so that the structure can be easier to transport and construct for offshore structures [3]. Curved SCS sandwich structure with slope is proposed as the ice-resisting wall to withstand the ice loading. Because sloping structures would encounter ice impact forces due to that the collided ice sheet would ride up the slope and fail in flexural bending rather than crushing as that occurred to a vertically sided structures, as shown in Figure 2. In this way, global ice load will be alleviated. The curved geometry also helps to optimize and improve the composite action. Furthermore, modular construction with rapid installation can be achieved, reducing the fabrication cost comparing to conventional RC structures [4].

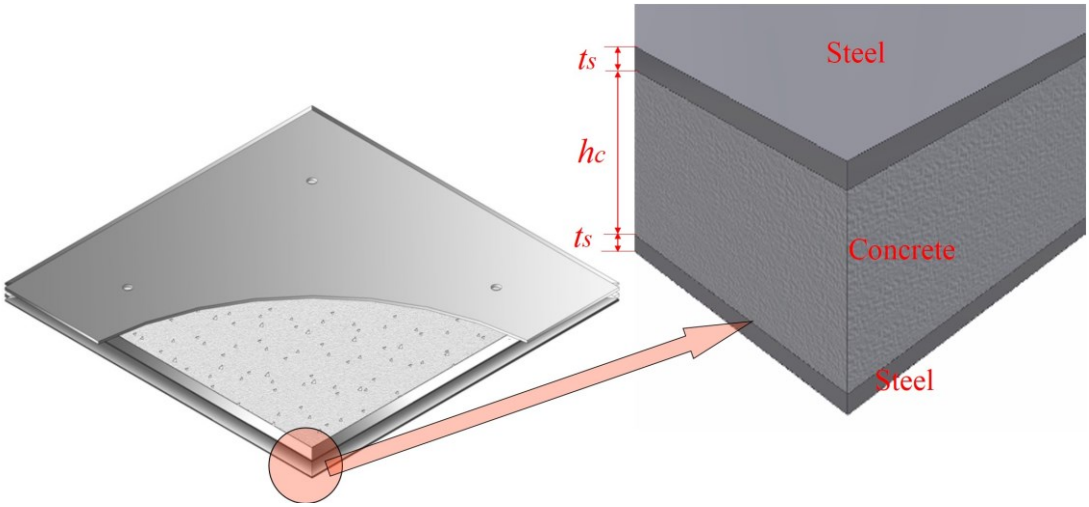

Figure 1: SCS sandwich composite structure infilled with concrete.

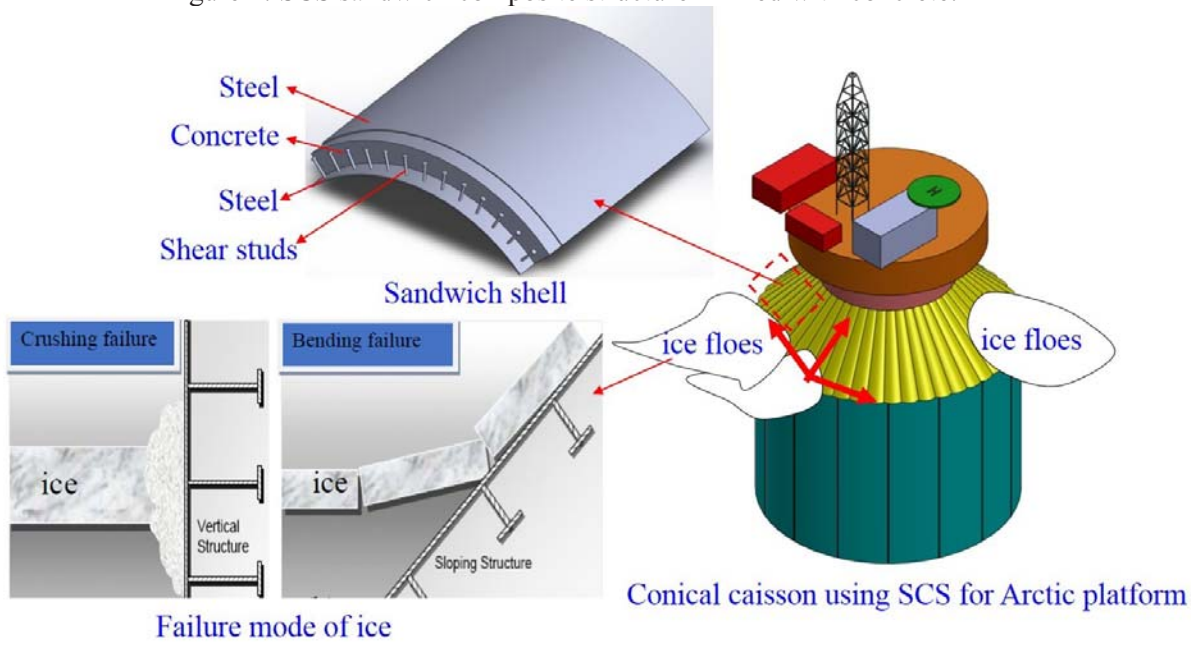

Figure 2: Gravity based arctic offshore caisson structure using SCS sandwich.

In this paper, multiple vaults of SCS sandwich shell were designed to resist ice contact pressure. Headed shear studs or novel J-hook connectors were introduced as mechanical connectors to construct the lightweight SCS sandwich panel. This paper firstly reported the development of new lightweight cement composite materials to be used as infilled core.

Mechanical properties of concretes were presented. Then, 20 curved SCS sandwich panels filled with ultra-lightweight cement composite were tested under patch load which aimed to investigate the beam-shear behavior of curved sandwich panels. The ultimate strength behavior of specimens were reported. Design equation was proposed to predict the shear resistances of the curved SCS sandwich panels by modifying Narayanan's equation. The accuracies of the design formulae were verified through comparing the tests results. Design recommendations were given based on the discussions and validations.

2 ULTRA-LIGHTWEIGHT CEMENT COMPOSITE INFILLED MATERIALS

One of the recent achievements in concrete technology is the development of ultra-lightweight cement composite (ULCC) and a floatable structural cement composite (FSCC) for marine and offshore application. The ULCC achieves a high compressive strengths of 60 MPa and high flexural strength of 8 MPa and hardening behavior with only 0.5% steel fiber added (by volume) when subjected to bending tests [1,5]. ULCC is a type of novel composites characterized by combinations of low densities, high compressive strength with specific strength of up to 47 kPa/kgm-3.

Table 1 shows the mix proportion of ULCC and Table 2 shows the mechanical properties of ULCC at age 28-day. Cylinder specimens with diameter of 100 mm and length of 200 mm were prepared to measure the compressive stress-strain curve and splitting tensile strength of ULCC at 28-day according to ASTM C39/39M [6] and ASTM C496/C496M [7] respectively. According to flow table test BS EN 1015-3 [8], around 200 mm flow is obtained. PVA fibers with length of 6 mm and diameter of 28 μm were added at a dosage of 0.5% by volume to prevent early shrinkage and increase the ductility and tensile strength of the ULCC.

Table 1: Mix proportion and design density of ULCC.

Water (kg/m^3)	OPC (kg/m^3)	SF (kg/m^3)	SRA (Liter)	Cenosphrere (kg/m^3)	Fiber (kg/m^3)	SP (Liter)	Design density (kg/m^3)
258.2	741.5	65.0	20.0	335.0	6.5	5.3	1380

OPC: ordinary Portland cement; SF: silica fume; SRA: shrinkage reducing admixture; SP: superplasticizer;

Table 2: Basic material properties of ULCC at age 28-day.

Material property	ULCC
Density after de-mould	1361 kg/m^3
Compressive strength cylinder f_{ck}	64 MPa
Ratio f_{ck}/ f_{cu}	1.01
Splitting tensile strength	5.4 MPa
Flexural strength	6.7-8 MPa
Static modulus of elasticity	15.4 GPa
Static Poisson's ratio	0.25

Floatable structural cement composite (FSCC) has a unit weight of less than 1000 kg/m^3 and 28-day compressive strength of up to 30 MPa, a major breakthrough in research in cement composite materials. Figure 3 shows a sample of FSCC when it is placed in water. It has

lower water absorptivity than that of normal weight concrete, which is essential to retain low unit weight in a marine environment. Table 3 shows the measured wet density after de-mould and compressive strength at age 28-day. However, so far only mechanical properties of FSCC cubs are studied and more investigations on FSCC are in process. It is expected that the use ULCC and FSCC enables SCS sandwich composite structures to be developed with lower self-weight, which will provide alternatives for Arctic platform construction and ship hulls. This will benefit the transportation and installation of pre-filled structures.

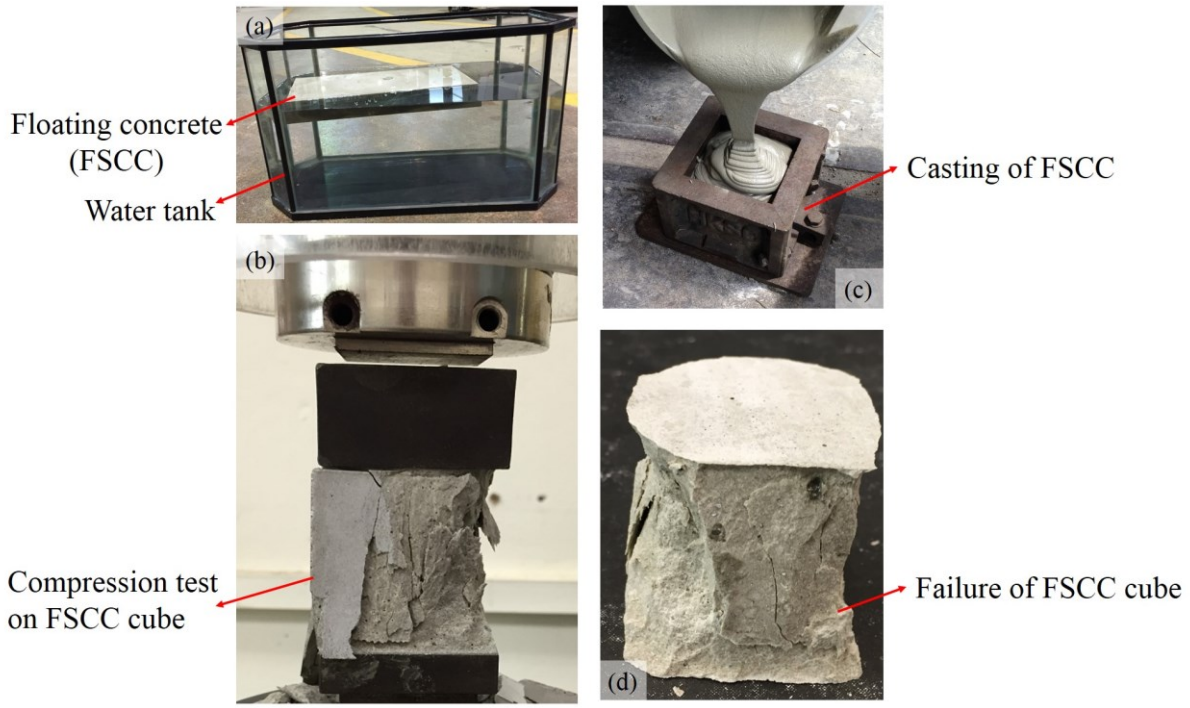

Figure 3: Floating concrete FSCC (a) sample in water (b) FSCC cube under compression (c) casting of FSCC (d) Failure of FSCC cube.

Table 3: Basic material properties of FSCC at age 28-day.

Item	Weight (g)	Volume (cm^3)	Density (g/cm^3)	Compressive strength (MPa)
FSCC-1	118.4	125	0.947	29.0
FSCC-2	118.7	125	0.950	28.1
FSCC-3	118.7	125	0.950	29.5
FSCC-4	119.9	125	0.959	30.3
FSCC-5	118.2	125	0.946	31.2
FSCC-6	121.1	125	0.969	32.3
Mean.			0.954	30.0
COV.			0.009	1.5

3 EXPERIMENTAL AND ANALYTICAL STUDY ON SANDWICH SHELLS

3.1 Test results and discussions

The ultimate strength behavior of SCS sandwich shells has been experimentally and numerically investigated [1, 9 and 10]. Figure 4 shows the details of the curved sandwich panels. The test results demonstrated all the failure modes and the related load-displacement

curves were captured and investigated. Parametric studies were conducted in which effect of rise-to-span ratio, span-to-thickness ratio, steel contribution ratio, degree of composite action, loading pattern and boundary conditions were considered. A unified deep model has been developed to predict the transverse shear resistance of the flat and curved SCS sandwich panels [11].

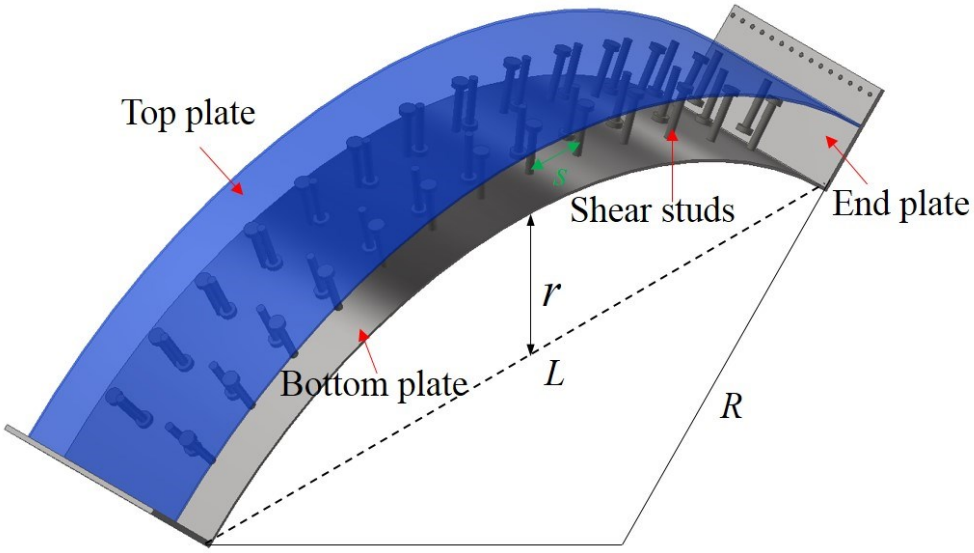

Figure 4: Typical curved sandwich panel with overlapped shear studs.

3.2.1 Failure modes

Failure mode is key proof to develop the ultimate strength model which can be identified by strain development, stress distribution and macroscopic collapse observations from the physical tests. The failure mode of curved SCS sandwich panels is significantly correlated to many factors, from the geometrical factors (rise-to-span ratio, span-to-thickness ratio, etc.) to loading patterns (e.g., pressure load, asymmetric pressure, punching load, load eccentricity, etc.). Geometrical conditions may change the stress flow from loading position to the part where is stiff so that leads to completely different failure mechanism. While the loading pattern may directly affect the failure path. For example, two types of ice load cases may govern the design of ice-resisting panels which are concentrated point load on a small area and lower pressure on larger area of the structure. For the former case, punching may be induced with three dimensional effects while for the latter case, flexural or shear failure (depends on the shear-span ratio) may occur with ignoring the plane strain effect. Figure 5 shows the possible failure modes of curved SCS sandwich panels.

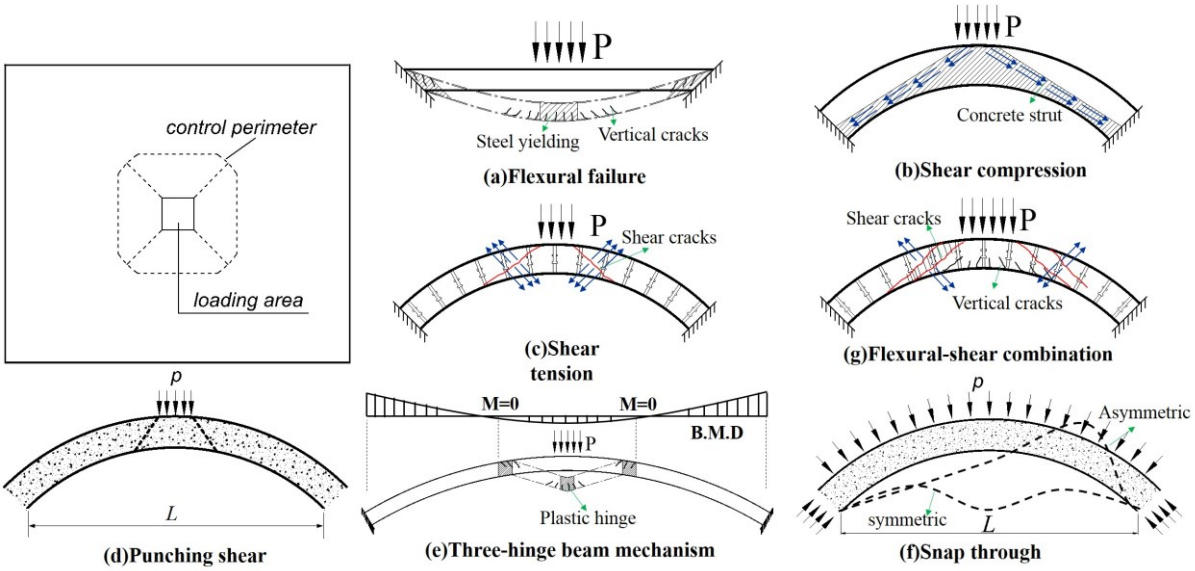

Figure 5: Possible failure modes of sandwich composite panels.

3.2.2 Design equations of sandwich panels

Failure mode is key proof to develop the ultimate strength model which can be identified by strain development, stress distribution and macroscopic collapse observations from the physical tests. The failure mode of curved SCS sandwich panels is significantly correlated to many factors, from the geometrical factors (rise-to-span ratio, span-to-thickness ratio, etc.) to loading patterns (e.g., pressure load, asymmetric pressure, punching load, load eccentricity, etc.). Geometrical conditions may change the stress flow from loading position to the part where is stiff so that leads to completely different failure mechanism. While the loading pattern may directly affect the failure path. Typically, there are five main failure modes observed from the analysis which are (1)~(5) below.

(1)Flexural failure (Figure 5a)

This failure initiates from yielding of tension plate in sandwich beam. The load-displacement curve exhibits an elastic stage and a ductile unloading behavior. Based on the plan section remain plan assumption and force equilibrium conditions of the sandwich section (shown in Figure 6), the flexural resistance of SCS sandwich beams with any type of shear connectors can be predicted by the following equations [12],

$$M_R = N_t(h_c + t_c/2 + t_t/2) + N_c(\lambda x/2) \tag{1}$$

where, $N_t = \min\left(n_t P_s, f_{yt} A_t\right)$, $N_c = \min\left(n_c P_s, f_{yc} A_c\right)$, $x = \dfrac{(N_t - N_c)}{\eta f_{ck} B \lambda x}$, $\lambda = 0.8$ for $f_{ck} \le 50MPa$, $\lambda = 0.8 - (f_{ck} - 50)/400$ for $50 < f_{ck} \le 90MPa$, referring to Euro Code 2. If the same thickness of top and bottom plate was used, $t_c = t_t = t$, the depth of neutral axis of bending section $x \approx 0$, resulting in

$$M_{pl} = n_p P_R (h_c + t) \tag{2}$$

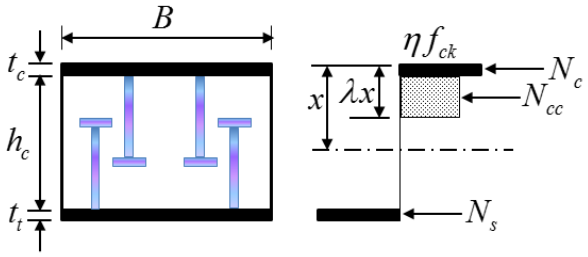

Figure 6: Force equilibrium of SCS sandwich section under bending.

(2)Beam-shear mode

This failure includes shear-compression (Figure 5b) and shear-tension (Figure 5c), is with a critical section extending in a plane across the entire width of the sandwich panels when the L/h_c ranges from 8 to 20 [1, 9]. Shear-compression failure initiates inclined cracks which would propagate to the whole beam section followed by crushing of diagonal concrete strut. Therefore, the maximum resistance is governed by the concrete failure which may be determined as follow:

$$V_c = f_{ce} A_{str} \tag{3}$$

where, A_{str} is effective area of the diagonal strut, which is defined as: $A_{str} = a_s \times b_w$, a_s is the effective depth of the diagonal strut while b_w is the beam width.

Shear-tension failure is characterized by a major crack developed with an inclined angle. Concrete strut crushing is not pronounced and typically, the specimen fails in concrete shear and pull-out of the shear studs. So the shear resistance is governed by concrete and shear studs. The shear studs act as shear links (stirrups) to resist the diagonal shear cracks developed in concrete core. Narayanan et al.[13] proposed a design method to predict the shear resistance of double skin composite beams as the following Eq.(4). However, this equation is applicable only for flat beams which ignores: (1) the effect of the rise-to-span ratio; (2) the effect of the top steel face plate and (3) overestimating the tensile resistance of the connectors embedded in concrete because the equation assumes that the shear stirrups (studs) yield all the time.

$$V = \frac{b f_{ck} h_c}{20\gamma_c} + \frac{0.5 n_0 A_s \sigma_u h_c}{s\gamma_a} \tag{4}$$

where f_{ck} is the compressive strength of concrete; h_c is the concrete core thickness; γ_c and γ_a are the partial safety factor for concrete and shear stud respectively (γ_c = γ_a=1.0 is used for validation); n0 is the number of shear stud connectors behave as the transverse shear stirrups distributed in the shear failure surface; $A_s\sigma_u$ is tensile resistance of the shear stud connectors in which σ_u is ultimate strength of studs and As is the cross-sectional area of the studs.

A modified shear model for curved sandwich panels was suggested as,

$$V = \frac{f_{ck}}{20\gamma_c} b h_e + \sum_{i=1}^{n_{cp}} \frac{T}{s} h_c \cos\alpha_i \tag{5}$$

where, T is the tensile resistance of shear connector embedded in concrete which can be determined by Eq.(6) [1]; s is the connector spacing; α_i is the angle between each stud axis and vertical axis.

$$T = \min \begin{cases} T_{cb} = 0.33\sqrt{f_{ck}} A_N \\ T_{pl} = 0.9\varphi f_{ck} e_h d \\ T_u = \phi A_{se} f_{ut} \\ T_{ps} = A_v f_u / \sqrt{3} \end{cases} \tag{6}$$

Considering the effect of the steel face plate, the effective height of the section needs to be modified as,

$$h_e = h_c + t\frac{E_s}{E_c} \tag{7}$$

$$\alpha_i = \frac{n_i s}{R}, \left(n_i = \{1, 2, ...n_{cp}\}\right) \tag{8}$$

where, R is the internal radius of the arch; n_i is the amount of shear studs linking the critical crack which equals to the number of shear studs welded to the bottom plate cross the crack band. Figure 7 illustrates the possible shear cracks origin from underneath the loading point to the point of inflection of the bending moment diagram in the arched member, therefore ni can be predicted by,

$$n_{cp} = \text{integer}\left(\frac{b}{s}\right) \cdot \text{integer}\left(\frac{R\beta}{s}\right) \tag{9}$$

where, integer $(\cdot)$ represents the integer of the term in bracket; b is breadth of the member, and β represents the included angle corresponding to the inflection point of bending moment diagram.

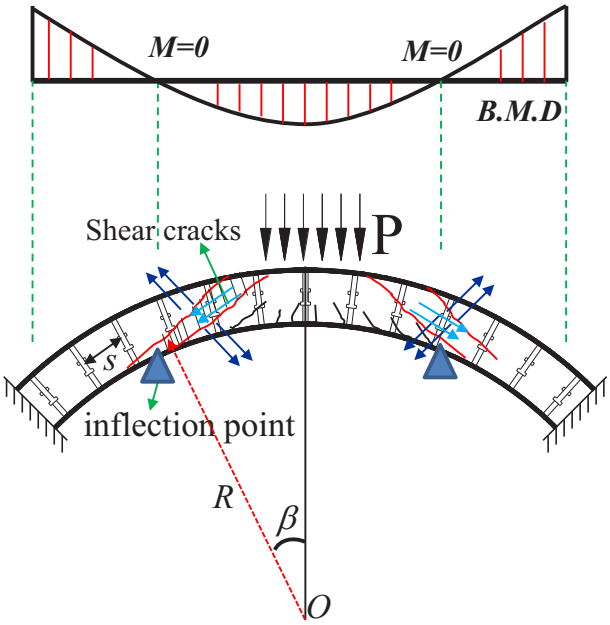

Figure 7: Possible shear cracks and inflection point.

(3)Punching shear failure

This failure is with a critical section extending around the perimeter of the loaded area (Figure 5d). Typically, a concrete frustum would form before the steel face plate is punched through. The punching shear resistance of lightweight concrete slabs or column bases is determined by summing the shear resistance provided by the concrete core and the contribution of the shear reinforcement as,

$$V = v_{Rd,cs} u_1 d \tag{10}$$

$$v_{Rd,cs} = 0.75 v_{Rd,c} + v_{Rd,s} \tag{11}$$

$$v_{Rd,c} = C_{lRd,c} k \eta_1 (100 \rho_1 f_{lck})^{1/3} + k_f \tau_{f,FRC} \tag{12}$$

where the basic control perimeter $u_1 = 2(L_a + L_b)$, $L_a = 2x$ which is obtained from making sectional bending moment $M_{arch}(x) = 0$ while L_b is obtained by $L_b = l_b + \frac{2h_c}{\tan\theta_{wid}}$.

Considering the different failure modes of headed shear studs in the concrete, the second term in Eq.(10) could be replaced by $v_{Rd,s}$ which is given by

$$v_{Rd,s} = \sum_{i=1}^{n_{cp}} \frac{\bar{h}_c}{s} F_t \frac{1}{u_1 \bar{h}_c} \sin\alpha_i \tag{13}$$

where n_{cp} is the amount of shear connectors linking the shear cracks which equals to the number of shear studs attached to the inner plate within the critical perimeter u_1 subtracting the number of shear studs under the loading area; α_i is the angle between each stud axis and vertical axis, which can be calculated by Eq.(8).

(4) Three-hinge beam mechanism

The failure mode may change to three-hinge beam mechanism if the L/h_c is larger than 20 (Figure 5e). However, the maximum pressure resistance in three-hinge beam mechanism is much lower than that subjected to other failures where the arch action is not imposed.

(5) Snap-through mode

If SCS shell is subjected to uniform pressure loading, failure mode may become stability mechanisms which are symmetric and asymmetric snap-through mode (Figure 5f). The pressure resistance of sandwich shell could be predicted using finite element analyses. Other than those, with L/h_c ratio between 12.5 and 20 (e.g., L/h_c=17), mix-mode is observed (Figure 5g). Asymmetric load condition causes a reduction in punching load resistance of the curved sandwich panel. It is found that the secant stiffness remains similar but the maximum resistance is lowered up to 25%, which proves that the asymmetric loading scenario is more critical and unfavorable compared to that of centrally loaded panel.

3.2 Validation of proposed equations

All the partial safety factors in the proposed formulae are taken as 1.0 for the comparison with test results. Table 5 compares the calculated and measured shear resistance of curved sandwich panels. The predictions by Eurocode 2 method [14], Narayanan's equation and modified Narayanan's equation are compared with 20 test results. It is found that the Eurocode 2 method and Narayanan's equation give about 33%-37% over-predictions compared to the test results. The average test-to-prediction ratio is 1.37 with a coefficient of variation (COV) of 0.23 for Eurocode 2 method while these values for Narayanan's equation are 1.33 and 0.20 respectively. However, the suggested model offers the average test-to-prediction ratio of 1.08 with a COV of 0.17. Therefore, the suggested model gives a reasonable description of the shear resistance of the curved sandwich panels with acceptable accuracy. Specifically, it should be noted that the suggested method over-predicts the resistance of FSB-01 and SB-01. This is because FSB-01 fails in the flexural mode and the flexural resistance is governed by yielding of steel face plate. While for SB-01, sliding of the supports are observed during the test. The premature severe separation between bottom face plate and concrete leads to lower shear resistance. This indicates that the structural behavior of curved sandwich panels is sensitive to the end supports which needs more investigations in the future. Therefore, FSB-01 and SB-01 are not included in the calculation of the mean value and COV in Table 5.

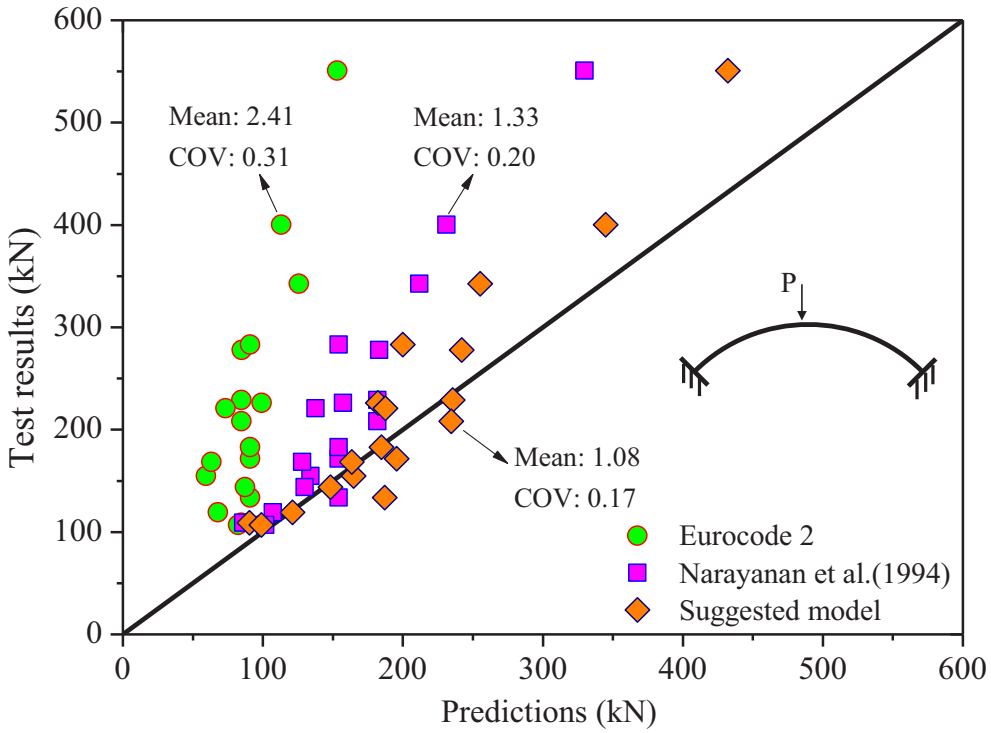

Figure 8: Comparison between test and predictions.

3.3 Benefit of using curved sandwich

Curved SCS sandwich panel can resist higher patch loads than that of a flat panel due to arching effect. Test and numerical results demonstrate that the failure mode may change to compressive related mode. Most of the part of the components are subjected to compression rather than bending so that they sustain less deflection compared to flat panels which would experience extensive deflection. This suggests that the curved sandwich panels are structurally more efficient in resisting ice pressure for Arctic offshore application. It should be noted that curved members are quite sensitive to the sliding of end supports which should be rigid design to prevent horizontal movement. This is can be guaranteed by using strong tie rods or cables to connect both end supports of curved SCS sandwich.

As a result, to improve the ultimate pressure resistance, it is recommended to utilize the arching effect. Based on the previous experimental and numerical studies [1, 2, 9, 11], to achieve high resistance and ductility behavior the optimal design parameters for the curved SCS sandwich panels subjected to patch load are summarized in Table 4.

Table 4: Optimal parameters for design of curved sandwich panels.

Parameters	Recommended value
Rise-to-span ratio (r/L)	0.15~0.2
Span-to-thickness ratio(L/h_c)	8~12.5
Steel contribution ratio ($A_s f_y/A_c f_c$)	0.5-0.8
Connector spacing (s)	$s \le 20 t_s \sqrt{235/f_y}$ (full composite)
Stud diameter-to-plate thickness (d/t_s) <2.5 (prevent punched-through of steel plates)	
End supports	Rigid joint by using tie rods or cables

4 COMPARISON WITH DESIGN GUIDES

To further investigate the ultimate strength behavior of SCS sandwich shells, 12 FE models were created and analyzed ABAQUS [9]. The primary investigated parameters included rise-to-span ratio (r/L), span-to-height ratio (L/h_c), loading position, loading area and composite action. Figure 8 depicts the interaction diagrams between design ice pressure given by ISO 19906 [16] and contact loaded area and compares with the performance of SCS sandwich shells subjected to different loading scenarios [2, 9, 11, 15 and 17-19]. The pressure resistance of sandwich shells obtained from experimental and numerical results are plotted in the chart, from small ice contact area (0.1 m^2) to larger contact area (32 m^2). In the chart, it is found that: (1) thin SCS sandwich cylindrical shells proposed by Shukry and Goode [19] cannot achieve sufficient resistance to satisfy the ISO 19906 requirement when scales up to a prototype size; (2) all the sandwich shells [1, 10, 17] and full-composite SCS sandwich plates [18] appear to satisfy the proposed ISO criteria. However, the partial-composite SCS sandwich plates and beams fail to sustain such applied ice contact pressure. Thus, full-composite structure is recommended for design of the SCS sandwich structure. To achieve full composition action, introducing mechanical shear connectors in the sandwich structures is the first choice for design purpose which plays essentially on improving the structural performances; (3) the flat panels fail in flexural mode has a lowest pressure resistance compared to that of sandwich shells fail in shear mode. This is because of the arching action which helps shell structures to enhance the resistance against the ice pressure load. The SCS shells are more superior in resisting ice contact pressure compared to flat panels.

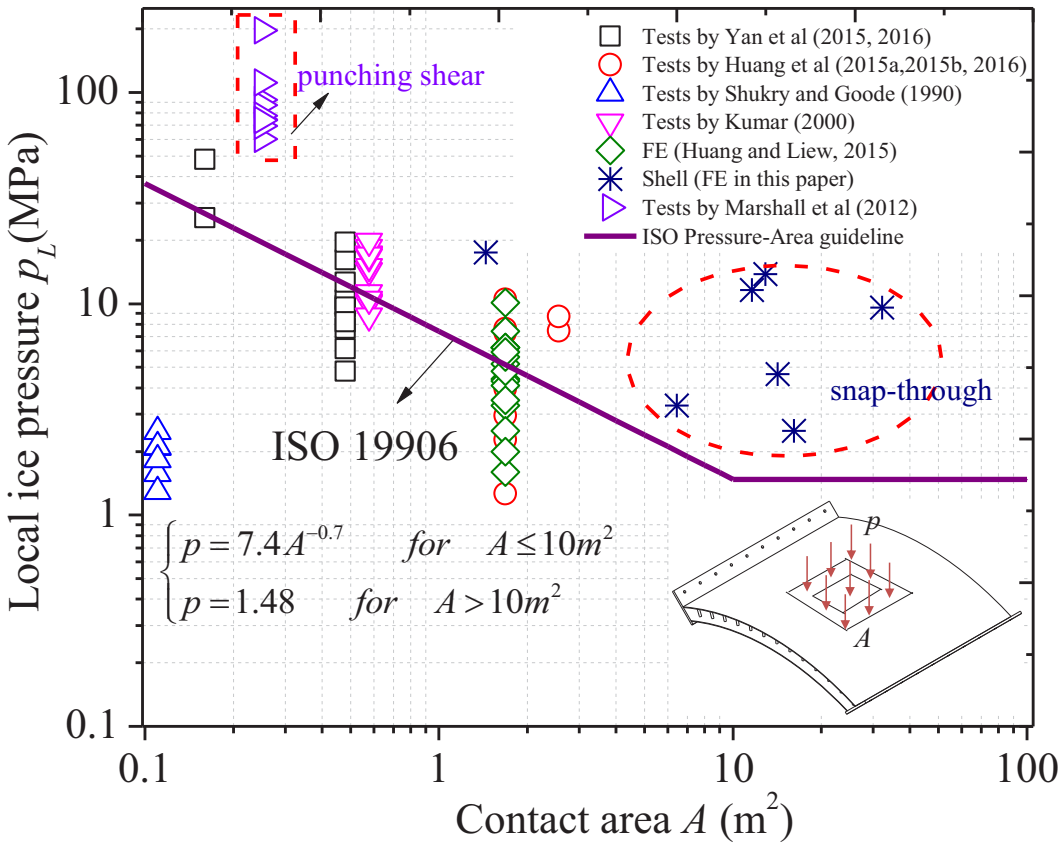

Figure 9: Resistance of experimental and numerical results V.S. ISO 19906 ice pressure.

5 CONCLUSIONS

This paper presents the novel Steel-Concrete-Steel (SCS) sandwich structures subject to patch load. Lightweight and high strength cement composite materials with density from 980-1500 kg/m^3 and compressive strength from 30-60 MPa are developed for the construction of sandwich composite structures. Steel-concrete-steel sandwich shell panel filled with ultra-lightweight cement composite is proposed for Arctic oil/gas production platform to resist the ice impact pressure. Experimental and analytical studies are carried out to investigate the structural behaviors of the SCS sandwich structures under quasi-static loads. Based on the experimental and analytical studies, the following conclusions can be drawn:

(1) Compared to steel stiffened plate structure, the proposed SCS sandwich structures can achieve higher strength-to-weight ratio and develop significantly higher flexural stiffness.

(2) Nonlinear finite element analyses were carried out to generate more data to supplement the limited test data on the SCS sandwich structures with different ice-contact pressure and areas. The numerical and the results show that the proposed composite SCS sandwich shells fail in snap-through mode, combined punching and flexural mode and they can be designed to satisfy the ISO criteria which provides further confidence for their use in the Arctic region.

(3) Design formulae have been developed to predict the flexural, shear and punching shear resistance of the SCS sandwich composite shells. The predicted results exhibit good correlations with the test and numerical results.

(4) Parametric studies have been carried and optimal range parameters are recommended for the design of curved sandwich panels: rise-to-span ratio = 0.15~0.2, Span-to-thickness ratio = 8~12.5, Steel contribution ratio = 0.5-0.8, and connector spacing $20t_s\sqrt{235/f_y}$. To prevent punched-through of steel plates, stud diameter-to-plate thickness d/ts <2.5 is suggested.

ACKNOLEDGEMENT

The research is supported by the National Research Foundation Singapore, Sembcorp Industries Ltd and National University of Singapore under the Sembcorp-NUS Corporate Laboratory.

REFERENCES

[1] Huang, Z.Y., Liew, J.Y.R., Xiong, M.X. and Wang, J.Y. (2015). “Structural behaviour of double skin composite system using ultra-lightweight cement composite.” *Construction and Building Materials*, 86, pp.51-63.

[2] Huang, Z.Y., Wang, J.Y., Liew, J.Y.R., Marshall, P.W. (2015). “Lightweight steel–concrete–steel sandwich composite shell subject to punching shear.” *Ocean Engineering*, 102, pp. 146-161.

[3] Huang, Z.Y., Palmer, A.C., Marshall, P.W, Liew, J.Y. R (2015). “Arctic platform constructions using steel-concrete-steel sandwich composite”, *23th International Conference on Port and Ocean Engineering under Arctic Condition (POAC)*, NTNU, Trondheim, Norway, June 14-18, 2015.

[4] Varma, A.H., Malushte, S.R., Lai, Z.C. (2015). “Modularity & innovation using steel-plate composite (SC) walls for nuclear and commercial construction”, *11th International Conference: Advances in Steel-Concrete Composite Structures (ASCCS)*, Beijing, China, Dec 3-5, 2015.

[5] Wang, J.Y., Chia, K.S., Liew, J.Y.R, Zhang, M.H. (2013). “Flexural performance of fiber-reinforced ultra-lightweight cement composites with low fiber content”. *Cement Concrete Composite*, 43, pp. 39-47.

[6] ASTM C39/C39M-09. “Standard Test Method for Compressive Strength of Cylindrical Concrete Specimens”.

[7] ASTM C496/C496M-11. "Standard Test Method for Splitting Tensile Strength of Cylindrical Concrete Specimens".

[8] BS EN 1015-3-1999. "Methods of Test for Mortar for Masonry".

[9] Huang, Z.Y, Liew, J.Y.R. (2015). "Nonlinear finite element modelling and parametric study of curved steel-concrete-steel double skin composite panel filled with ultra-lightweight cement composite". *Construction and Building Materials* 2015; 95, pp.922-938.

[10] Yan, J.B., Liew, J.Y.R, Qian, X.D., Wang, J.Y. (2015) "Ultimate strength behavior of curved steel-concrete-steel sandwich composite beams". *Journal of Constructional Steel Research*; 115, pp.316-328.

[11] Huang, Z.Y., Liew, J.Y.R. (2016). "Experimental and analytical studies of curved steel-concrete-steel sandwich panels under patch loads". *Materials & Design*, 93, pp.104-117.

[12] Liew, J.Y.R., Sohel, K.M.A. (2009). "Lightweight steel-concrete-steel sandwich system with J-hook connectors". *Engineering Structures* 31, pp. 1166-1178.

[13] Narayanan, R., Roberts, T.M., Naji, F.J. (1994). "Design guide for steel–concrete–steel sandwich construction, Volume 1: General principles and rules for basic elements", The Steel Construction Institute, Ascot, Berkshire, UK.

[14] Eurocode 2 (2004). "Design of concrete structures-Part 1-1: General rules and rules for buildings". BS EN 1992-1-1.

[15] Marshall, P., Sohel, K., Liew, R.J., Yan, M., Palmer, A.C. and Choo, Y.S. (2012). "Development of SCS composite shell for Arctic caissons." *Proceedings, Arctic Technology Conference*, Houston, paper OTC23818.

[16] BS EN ISO 19906 (2010). "Petroleum and Natural Gas Industries-Arctic Offshore Structures", BSI Standards Publication.

[17] Yan, J.B., Liu, X.M., Liew, J.Y.R., Qian, X.D., Zhang, M.H. (2016). "Steel–concrete–steel sandwich system in Arctic offshore structure: Materials, experiments, and design". Materials & Design 91, pp. 111-121.

[18] Kumar, G., "Double skin composite construction". M. Eng. Thesis National University of Singapore, Singapore, 2000.

[19] Shukry, M.E.S., Goode, C.D. (1990). "Punching shear strength of composite construction". *ACI Structural Journal*. 87(1), pp. 12–22.